ethanol and one crystallization from 95% ethanol gave 21.5 g. (66%) of product which melted at 83–85°. Another crystallization did not improve the melting point.

Anal. Calcd. for $C_{28}H_{28}OSi$: Si, 6.84. Found: Si, 7.19.

Cleavage of Tribenzyl-*p*-anisylsilane.—The cleavage of 8 g. (0.0195 mole) of the silane in 40 cc. of glacial acetic acid was carried out in the usual manner. After fifteen hours the solution was cooled and 3.2 g. of a colorless solid was filtered off. This material melted at 131–134° and was evidently slightly impure tribenzylsilyl chloride. It was placed in 20 cc. of water and was allowed to stand overnight to give 2.9 g. of tribenzylsilanol which melted at 101.5–103.5° and did not depress the melting point of an authentic sample.

The acetic acid solution was added to about 50 cc. of water and was steam distilled to remove the anisole. The residue in the flask deposited crystals which, after purification from a chloroform–petroleum ether (b. p. 60–68°) mixture, proved to be 2 g. of the silanol with a melting point of 103–104°. Thus, the total silanol isolated was 4.9 g. (79%).

The steam distillate was extracted with ether and the combined extracts were washed with dilute sodium carbonate solution and dried over sodium sulfate. Removal of the ether and distillation of the residue gave 1.8 g. (84%) of anisole which was identified as the 2,4-dinitro derivative.

Cleavage of Tetra-*o*-tolyldisilanediol.—The cleavage of 5 g. (0.011 mole) of the diol, prepared according to the procedure of Smart,[21] in 35 cc. of acetic acid was carried out in the usual manner during fifteen hours. After about thirty minutes the reaction mixture deposited a white solid which remained throughout the course of the reaction and was filtered off at the end. This material did not melt, showed only a very slight darkening when heated, and was immediately dissolved by hydrofluoric acid. It weighed 1.3 g. and was thus a quantitative yield of silica.

The material which had collected in the cold trap was added to 20% sodium carbonate solution and, after extraction, drying and removal of the ether, there was obtained 1.7 g. of liquid of rather indefinite boiling point which was identified as toluene by conversion to 2,4-dinitrotoluene. This represents a 43% yield of toluene based on the removal of all four of the groups.

Distillation of the acetic acid from the reaction mixture did not leave any residue. Attempted nitration of the toluene, which co-distilled, by four hours of refluxing of the acetic acid solution with 8 cc. of fuming nitric acid was unsuccessful, only a very small amount of material which appeared to be crude *p*-nitrobenzoic acid being obtained.

(21) Smart, unpublished studies, Iowa State College.

Acknowledgment.—The authors are grateful to Dr. Robert A. Benkeser and William J. Meikle for their assistance.

Summary

Organosilanes have been shown to undergo cleavage by anhydrous hydrogen chloride, a reaction characteristic of organometallic compounds. The order of ease of removal of radicals is in essential agreement with the series previously established with organic derivatives of mercury and lead.

AMES, IOWA RECEIVED DECEMBER 4, 1948

[CONTRIBUTION FROM THE DEPARTMENT OF CHEMISTRY OF THE UNIVERSITY OF ROCHESTER]

Pore Structure in Activated Charcoal. I. Determination of Micro Pore Size Distribution

BY A. J. JUHOLA[1,2] AND EDWIN O. WIIG

I. Determination of Micro Pore Size Distribution

A knowledge of the pore size distribution is important in the evaluation of charcoals as catalyst carriers and in the interpretation of physical adsorption. The need for such knowledge in the development of better gas mask charcoals prompted a search for a method of determining pore diameters and volumes. During the period December, 1943, to July, 1945, a practical method was developed at the Division 10 Central Laboratory of the National Defense Research Committee at Northwestern Technological Institute. Since then a more fundamental study of pore structure has been continued in this Laboratory in an attempt to clarify the many points of uncertainty in the method.

Briefly, to determine a complete pore size distribution curve four quantities need to be determined (1) Total Pore Volume, which is equal to the volume of the charcoal by mercury displacement minus the volume of the charcoal by helium displacement, (2) Submicro Pore Volume, which is equal to the volume of charcoal by liquid water displacement minus the volume of the charcoal by helium displacement, (3) Micro Pore Size Distribution by application of the Kelvin equation to the desorption side of the water adsorption isotherm, and (4) Macro Pore Size Distribution, by measuring the quantities of mercury forced, at known pressures, into the pores of the charcoal. The sum of the submicro, micro and macro pore volumes makes up the total pore volume. The micro pore diameter range is believed to be between 10 and 30 Å. and the macro pore range between 30 and 100,000 Å. It was first thought that the submicro pore volume was the volume of pores below about 10 Å. but experimental evidence obtained later seems to indicate that it is not due to small pores but to void space between sorbed water molecules, since the closest packing cannot be attained in pores whose diameters are only 2 to 10 molecular diameters. The present paper, the first of a series concerned with pore size and pore distribution in charcoal, deals with the applica-

(1) From a thesis submitted to the Graduate School of the University of Rochester in partial fulfillment of the requirements of the degree Doctor of Philosophy.

(2) Present address: The Barrett Division, Allied Chemical and Dye Corporation, Philadelphia, Pennsylvania.

tion of the Kelvin equation to the water isotherm to determine the micro pore size distribution.

Calculation of the Micro Pore Size Distribution from the Water Adsorption Isotherm.—To calculate the pore diameter D from the relative vapor pressure P/P_0, the Kelvin[3] equation has the form

$$D = \frac{4V\sigma \cos\theta}{RT \ln P/P_0} \qquad (1)$$

where V and σ are the molar volume and surface tension, respectively, of the adsorbed water and θ is defined as the contact angle of the water meniscus with the pore wall. If it is assumed that water is adsorbed by capillary condensation, evidence for which has been presented,[4] and that the Kelvin equation is a valid expression for the dependence of the relative vapor pressure on the pore diameter, it is necessary to determine V, σ and θ before the equation can be properly used. In this study of pore structure σ is assumed to have its normal value and V is measured by helium displacement as described previously.[4] The principle on which the determination of θ is based is simple but the experimental procedure becomes quite involved. If water is adsorbed in pores in bulk liquid phase with very little surface adsorption, then the volume of water also represents pore volume. With this pore volume is associated surface area. If the pores are regarded as cylindrical segments, then for segments of diameter D the pore volume v, and the surface area A are related by the equation

$$D = 4kv/A \qquad (2)$$

where k is the conversion factor of units of measure. If water is desorbed or adsorbed in small increments and after each desorption or adsorption the surface area is determined, a curve may be plotted showing the variation of surface area with change in occupied pore space. The reciprocal of the slope of this curve at any pore volume is dv/dA and may be substituted into equation (2) for v/A. With this information a pore size distribution curve (D *vs.* v) may be constructed. The magnitude of θ is determined by assigning it a value which will give the best agreement between the pore diameter calculated by the Kelvin equation and the corresponding experimentally determined pore diameters.

Experimental

Materials.—During the course of the work 140 different water adsorption isotherms were obtained on as many different charcoal samples of all kinds. Of these isotherms 14 were selected as typical. The latter[5] were found to fall into three groups, leading to the selection, for detailed study, of three charcoals, the water and nitrogen adsorption isotherms of which are shown in Figs. 1 and 2. Charcoal N-291-AY-1, which is a zinc chloride-activated wood charcoal, has an isotherm characterized by small adsorption at low and high relative pressures with practically all the adsorption occurring in the intermediate relative pressures range. Charcoal Darco G-60, an activated wood charcoal, adsorbed most of the water at relative pressures above 0.90. Charcoal PN-439 is a baked material processed from briquetted coal but unactivated. Its isotherm is characterized by relatively large adsorption at very low relative pressures, a feature which may be attributed to monolayer adsorption. Charcoals N-291 and PN-439 are granular, 16–20 mesh, while the other is a very finely divided material.

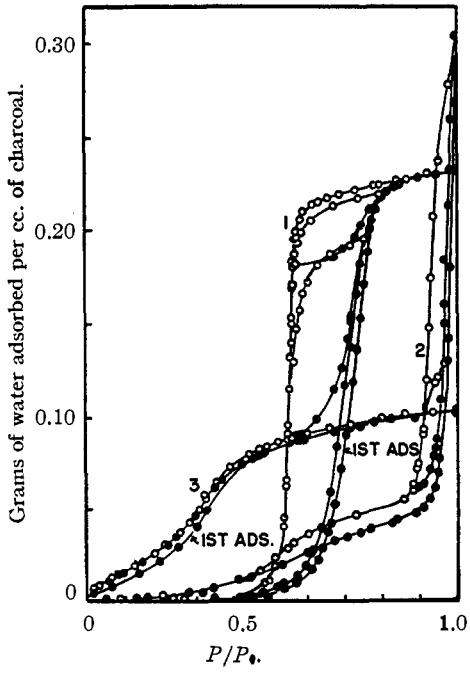

Fig. 1.—Water adsorption isotherms at room temperature: 1, N-291; 2, Darco G-60; 3, PN-439; O desorption; ● adsorption.

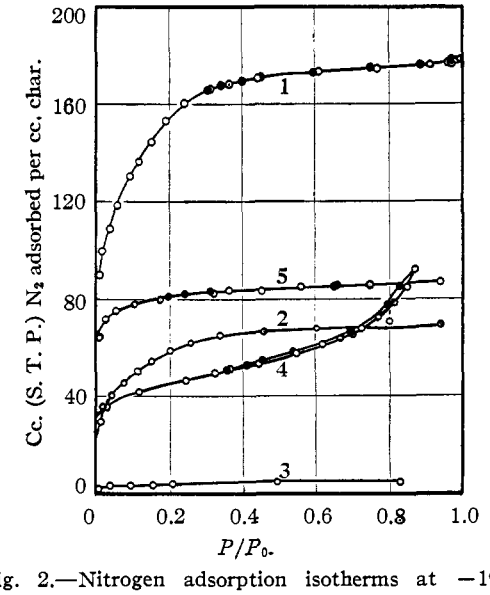

Fig. 2.—Nitrogen adsorption isotherms at −195°: O adsorption; ● desorption; 1, N-291; 2, N-291 plus 0.130 g. adsorbed H_2O per cc. char; 3, N-291 plus 0.214 g. adsorbed H_2O per cc. char; 4, Darco G-60; 5, PN-439.

(3) Thompson, *Phil. Mag.*, [4] **42**, 484 (1871).

(4) Wiig and Juhola, THIS JOURNAL, **71**, 501 (1949).

(5) Juhola, Ph.D. Thesis, University of Rochester, 1947.

The method for determining the water adsorption isotherms has been described previously.[4]

Determination of Surface Area–Pore Volume Curve.—This involved three types of experimental measurements: (1) the measurement by nitrogen adsorption of the surface area of the original charcoal by the BET method[6]; (2) the cooling to −195° of a sample of charcoal containing adsorbed water without altering the nature or position of the adsorbed water and again measuring the surface area by the nitrogen adsorption method; and (3) the measurement of the density of the water as held by the charcoal at −195°.

To minimize migration of the adsorbed water while cooling the charcoal to −195°, it was cooled in stages in helium at one atmosphere pressure.[4] The sample was held at ice temperature for several hours, then cooled to Dry Ice temperature and held there for about five hours, and finally submerged in liquid nitrogen. After attaining equilibrium at −195°, the helium was pumped off for one hour and the sample was ready for helium displacement and nitrogen adsorption measurements. To check the effectiveness of this procedure the sample was warmed in a similar manner to Dry Ice temperature and evacuated to remove the last traces of helium, then warmed to ice temperature and finally to 24°. The relative vapor pressure now was found to have shifted slightly toward the opposite side of the hysteresis loop, but judging from the "scanning the loop curves" this displacement involved only a small amount of water, from which it was concluded that practically all the water remained in its original position.

It was necessary to determine the volume of the adsorbed water at −195° since it is highly probable that its density at this temperature is not the same as at 24°. The apparatus used in making this determination, as also for nitrogen adsorption, was the same as that[4] used in determining the adsorbed volume at 24°, and the procedure was similar except that a correction for temperature and adsorbed helium replaced the water vapor pressure correction. The temperature was measured to within ±0.01° with an oxygen thermometer. Errors were minimized by keeping the liquid nitrogen level at the section of capillary tubing in the neck of the adsorption bulb.

These methods for measuring volumes were tested with only pure water in the adsorption tube. The density of water at 24° was measured as 0.997 which agrees with the accepted density at that temperature. At −195° the density was found to be 0.934 which is slightly higher than the value of 0.917 for ice at 0°. Most of this difference can be accounted for by thermal contraction. The surface area was negligible, hence no correction for adsorption of helium was necessary.

The surface areas by nitrogen adsorption were at first calculated by the "n" form of the BET equation, the value of n being determined by the method of Joyner, *et al.*[6] For N-291 dry or with 0.13 g. water per cc. char, C is ~ 430, $n = 1.2$; and with 0.214 g. water n is 2, while for Darco G-60 n varied from 2.7 to 7. With $n = 1.2$ on N-291 the straight portion of the BET plot falls in the range $P/P_0 = 0.01$ to 0.07 and with $n = 2$ from 0.03 to 0.3. For $C \sim 100$ and small values of P/P_0 (~ 0.05) the "n" form of the BET equation reduces essentially to the $n = \infty$ form. Furthermore, Joyner, *et al.*, found the "n" form did not agree with their experimental isotherms at relative pressures below 0.1 and greater than about 0.4. For these reasons and others indicated below the $n = \infty$ form was used in the present calculations.

Apparent "dead space" measurements by helium displacement at liquid nitrogen temperatures when varied amounts of nitrogen were adsorbed favored the areas obtained by the $n = \infty$ equation. If helium adsorption is proportional to surface area not covered by nitrogen, then when only a small part of the surface is covered the volume of helium adsorbed would be relatively large and, hence, the "apparent dead space" would be large. As the surface is gradually covered by adsorbing more nitrogen the volume of helium adsorbed would decrease, and finally at completion of the monolayer (V_m cc. of nitrogen adsorbed) the helium adsorption should be small. On plotting the apparent dead space volume against the volume of nitrogen adsorbed one might anticipate a change in slope at V_m. Such proved to be the case,[5] and the change in slope occurred at values of V_m in better agreement with values obtained by the $n = \infty$ rather than the "n" equation. Also, the constancy of cos θ (indicated later) was better using these values of the area. On dry N-291 V_m was 116 cc. by the $n = \infty$ form and 171 by the "n" form which, as mentioned above, does not hold below relative pressures of 0.1. On char PN-439 the two methods gave 71 and 76 cc., respectively, and on Darco G-60 both gave 37 cc..

This uncertainty in the magnitude of the surface areas determined by the BET method arises from the assumption that successive layers may have the same number of molecules as the first. This condition is not met in charcoals having cylindrical pores 10 to 20 Å. in diameter, where adsorption in the second or third layers is restricted to a much smaller number of molecules than in the first. The result of this restriction is that the BET equation is applicable in some cases only at low relative pressures, between 0.01 and 0.08, where the monolayer is approaching completion and the heat of adsorption is approaching a constant value but adsorption in the second layer is still negligible. Experimentally it has been observed in this study of pore structure that the BET plot has a straight portion at low relative pressure when the charcoal is known to have a large volume of small pores. For charcoals having larger pores the straight portion becomes longer and in one case (Darco G-60) it extended from 0.01 to 0.22 relative vapor pressure. Some of the surface areas reported in this paper were determined from BET plots extended to low relative pressures (*ca.* 0.01), although most investigators use the BET equation at relative pressures only above 0.05 or 0.1. Experience in this study indicates that such use of the BET equation is justifiable.

Results and Discussion

The volume curves of adsorbed water at 24° and −195° for the three charcoals studied are presented in Figs. 3, 4 and 5. For each charcoal at P/P_0 very close to unity, where helium adsorption is negligible or requires only a slight correction, the difference in volume at 24° and −195° can be accounted for by the difference in densities, 0.997 and 0.934, at these two temperatures. In calculating the adsorbed volume from the helium displacement measurements at −195° the volume of helium adsorbed was corrected for by assuming the amount adsorbed proportional to the surface area as measured by nitrogen adsorption at −195°. Dividing the BET V_m value into the volume of helium adsorbed by the dry charcoal at −195° gives the correction factor, or $\frac{0.405 \text{ cc.}}{V_m} = 0.00350$. The corrected volume curve at −195° for N-291 appears reasonable, being slightly above and almost parallel or converging slightly with the volume curve measured at 24°. The similarly corrected volume curves for the other two charcoals show anomalous behavior. The minimum in the curve in Fig. 5 has been found, upon further investigation, to be due to screening out of nitrogen molecules. This screening, however, was not due to small pores acting as

(6) Emmett in "Advances in Colloid Science," E. O. Kraemer, Editor, Interscience Publishers, Inc., New York, N. Y., 1942; Brunauer, Emmett and Teller, THIS JOURNAL, **60**, 309 (1938); Joyner, Weinberger and Montgomery, THIS JOURNAL, **67**, 2182 (1945); Emmett, THIS JOURNAL, **68**, 1784 (1946).

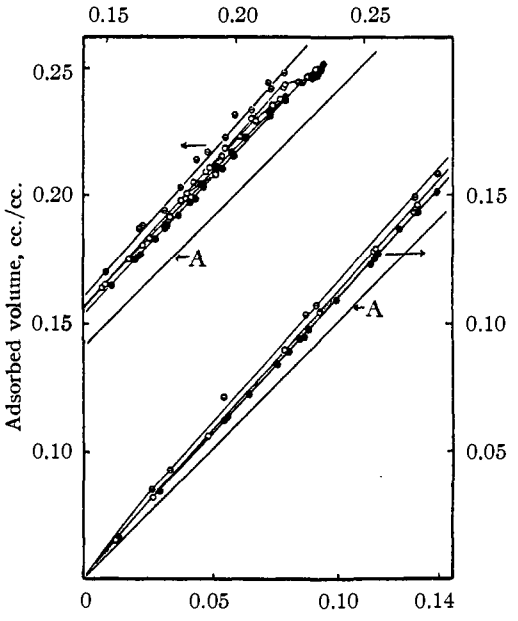

Fig. 3.—Volume of adsorbed water on charcoal N-291: ● adsorption and O desorption at 24°; ◒ adsorption and ⊖ desorption at −195°, corrected for helium adsorption (factor = 0.00350); A, normal volume of water.

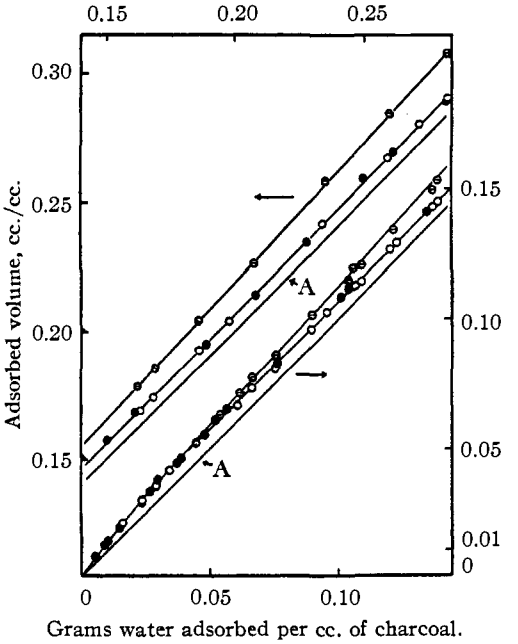

Fig. 4.—Volume of adsorbed water on Darco G-60: ● adsorption and O desorption at 24°; ⊖ desorption at −195°, corrected for helium adsorption (factor = 0.00302); A, normal volume of water.

a molecular sieve but to a decrease in the effective diameter of the opening remaining in the pores after a monolayer of water had been adsorbed. To obtain what might be the true vol-

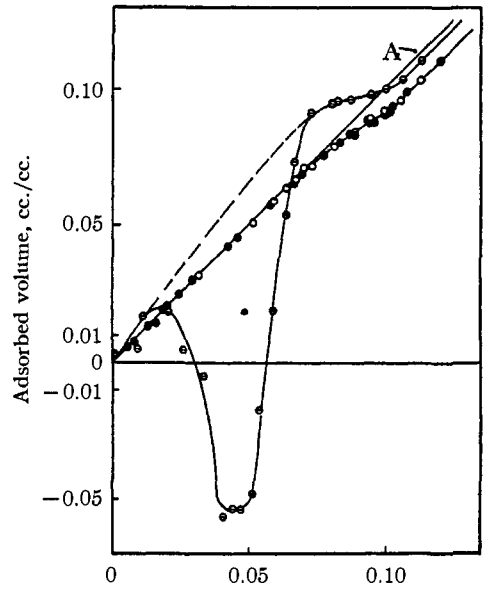

Fig. 5.—Volume of adsorbed water on PN-439: ● adsorption and O desorption at 24°; ⊖ desorption at −195°, corrected for helium adsorption (factor 0.00489); A, normal volume of water.

ume curve, the broken line curve was drawn between the points at 0.010 and 0.80 g. of water. In the case of Darco G-60, the volumes corrected for helium adsorption are too large if one uses the factor 0.00590, obtained by dividing the BET V_m into the volume of helium adsorbed by the dry charcoal. The discrepancy is associated with the pores which are filled by the first 0.01 g. of water adsorbed, since above this moisture content helium adsorption appears to be proportional to V_m but too large by a constant factor. It is in the direction to make it appear as though the helium adsorption was much greater or the nitrogen adsorption much less than it should have been during adsorption of the first 0.01 g. of water. If it is assumed that the first 0.01 g. of water is adsorbed by pores less than 10 Å. in diameter, a reasonable explanation of this discrepancy may be had if one takes into consideration the relative sizes of the nitrogen molecule, the helium atom, and the pore diameter. It can be shown that owing to packing effects in these small pores the surface area as calculated from nitrogen adsorption is less than 45% of the true surface area but the surface area available to the helium atoms, which are considerably smaller than nitrogen molecules, is much greater than this. For larger pores the surface areas available for each gas begin to approach each other. This explanation is consistent with observations and calculations made from the surface area–pore volume and pore size distribution curves. For the purpose of obtaining a surface area–pore volume curve the correction factor 0.00302 was chosen to give an adsorbed volume

curve which will converge with the curve determined at 24° at low moisture contents in a manner similar to that observed for charcoal N-291.

The volume curves of the adsorbed water at 24° for the latter have already been discussed in the previous publication,[4] in which the similarity between the volume curves and the isotherm was pointed out. This dependence of the adsorbed volume on the relative vapor pressure was attributed to capillary action. Hysteresis loops in the adsorbed volume curves for Darco G-60 and PN-439 are not apparent because of the narrowness of the hysteresis loop in the isotherms themselves, although the curves for both charcoals have a hump as would be expected from the isotherms.

The adsorbed volume curve at 24° for PN-439 (Fig. 5) coincides up to 0.070 g. of water with the normal curve but at higher moisture contents falls below it. At 0.105 g. of moisture content the adsorbed volume is 0.095 cc., which gives the adsorbed water an average apparent density of 1.16, a value considerably greater than the normal density. It is unusual for the adsorbed water in charcoal to have a density greater than 1.0; the adsorbed water on N-291 and G-60 have densities considerably less than 1.0.

The high density suggested the possibility of surface adsorption on this charcoal, and such a supposition is consistent with the unusually strong adsorption at low relative pressures. However, it would be expected that under these conditions the adsorbed volume curve should have gone below the normal curve at very low moisture contents. Since it did not occur there but at a much higher moisture content, 0.070 g., one may conclude that surface adsorption and capillary condensation occur simultaneously below this point, with surface adsorption predominating. Up to 0.070 g. the capillary action and the surface attraction compensate each other (compare preceding paper)[4] and the adsorbed volume fortuitously is equal to the normal volume, but at higher moisture contents the capillary action decreases and the water contracts as it did on N-291 and Darco G-60.

To substantiate this argument, adsorbed volume measurements were needed on a finely divided non-porous adsorbent in which no capillary adsorption is possible and which also strongly adsorbs water at low relative pressures. Studies by Harkins and Jura[7] on finely divided titanium oxide showed that water is adsorbed on this material by multilayer adsorption, and hence was suitable for this study. The volume curve determined for adsorbed water on titanium oxide at 24° is presented in Fig. 6. From these results it may be in-

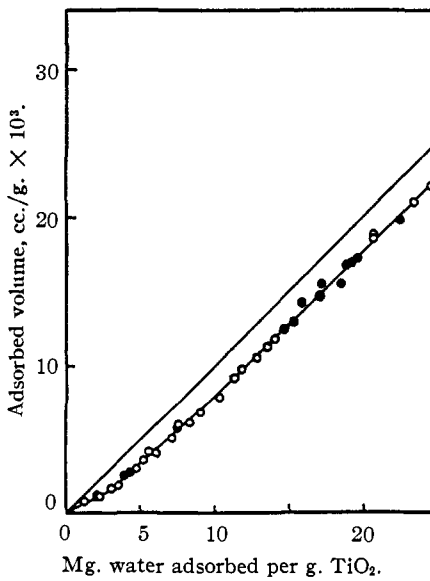

Fig. 6.—Volume of adsorbed water on finely divided TiO_2 at 24°: ● adsorption, O desorption; upper curve, normal volume.

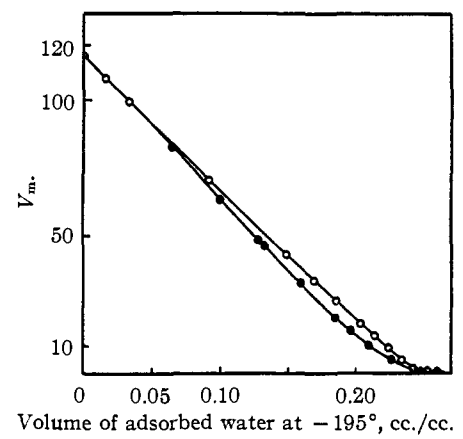

Fig. 7.—Surface area–pore volume curves for N-291: V_m, the volume of nitrogen, cc. per cc. char (S. T. P.), necessary to form a monomolecular layer on the carbon surface; ● adsorption and O desorption sides of water isotherm.

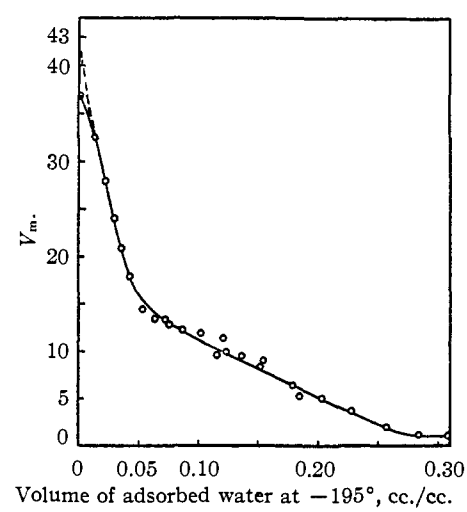

Fig. 8.—Surface area–pore volume curve for Darco G-60, desorption branch of the water isotherm.

(7) Harkins and Jura, THIS JOURNAL, 66, 919 (1944).

ferred that the adsorbed volume curve in Fig. 5 did not go below the normal curve at very low moisture content due to the counter effect of capillary action.

In Figs. 7, 8 and 9 are the surface area–pore volume (*i. e.*, adsorbed volume) curves of the three charcoals. The pore volume values were obtained from the adsorbed volume curves, measured at −195°, in Figs. 3, 4 and 5. After each desorption or adsorption of water V_m was measured. The discrepancy discussed in connection with the adsorbed volume curves measured at −195° for Darco G-60 appears in the upper end of the surface area–pore volume curve Fig. 8. The curve turns over slightly and meets the V_m axis at 37, but if the curve is extrapolated from points at pore volumes greater than 0.20 cc. the curve meets the V_m axis at about 43 cc. The surface area redetermined from the pore size distribution curve of this carbon agrees more closely with the surface area calculated from V_m equal to 43 cc. than to 37 cc. The curve for PN-439 (Fig. 9, obtained from the dotted curve, Fig. 5) is not a true surface area–pore volume curve because a large part of the water, being adsorbed in a monolayer, does not represent pore volume in the sense used here. This conclusion is further substantiated by comparing the curve for PN-439 with those for N-291 and Darco G-60. Up to 0.05 cc. the curve (Fig. 9) for

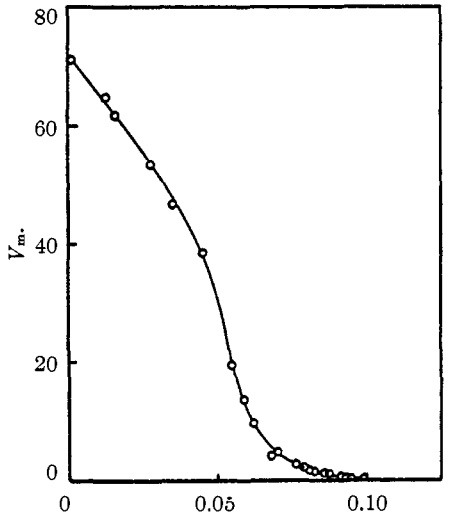

Fig. 9.—Surface area as a function of the volume of adsorbed water on PN-439, desorption side of the water isotherm.

PN-439 is concave and above 0.05 cc. is convex to the volume axis while the curves (Figs. 7 and 8) for N-291 and Darco G-60 are convex practically their full lengths, as required by the capillary condensation theory. Monolayer adsorption of water in capillaries followed, after the preceding layer is completed, by a second or third layer requires that the curve be concave.

In Figs. 10 and 11 are the pore size distribution curves in the micro pore range for N-291 and Darco G-60 calculated from the reciprocal of the slopes, dV/dV_m, of the curves in Figs. 7 and 8. For N-291 it was possible to determine two pore size distribution curves, one corresponding to each side of the hysteresis loop. The surface area–pore volume curve for PN-439, for reasons already stated, did not yield a valid pore size distribution curve.

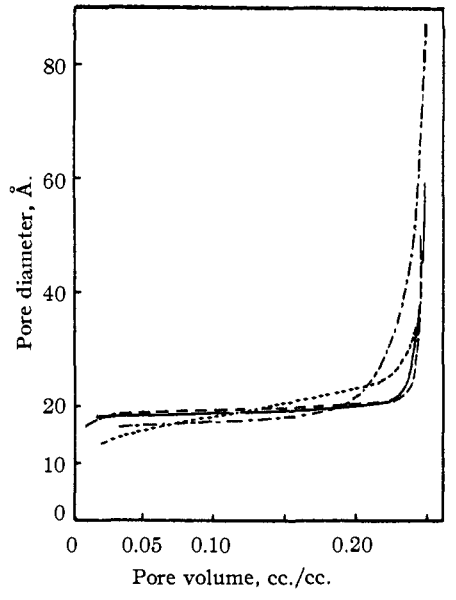

Fig. 10.—Pore size distribution in the micro pore range of N-291: — experimental desorption; —·— experimental adsorption; — — calculated Kelvin equation, desorption, cos θ = 0.49; · · · · · calculated Kelvin equation, adsorption, cos θ = 0.28.

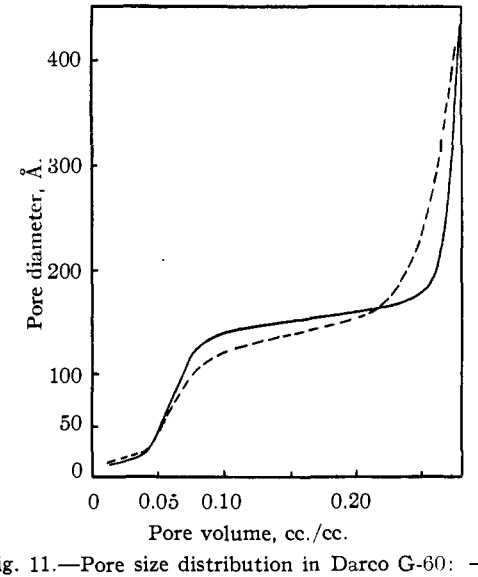

Fig. 11.—Pore size distribution in Darco G-60: — experimental desorption; - - - - calculated Kelvin equation, desorption, cos θ = 0.49.

In Tables I, II and III are summarized the steps in the calculation of cos θ for N-291 and Darco G-60. In column 1 are the pore volume intervals at which calculations were made. In column 2 are the weights of adsorbed water corresponding to the volumes in column 1, obtained from the curves in Figs. 3 and 4. The molar volumes, V, in column 3 were calculated from the values in columns 1 and 2. The relative vapor pressures in column 4 corresponding to the weights in column 2 were obtained from the isotherms in Fig. 1. In column 5 are pore diameters calculated with the Kelvin equation when cos θ = 1.0, T = 297.1°, R = 8.315 × 10^7 ergs per mole per degree, σ = 72.7 dynes per cm., and using values of V and P/P_0 from columns 3 and 4, respectively. When these pore diameters are divided into the corresponding pore diameters in the experimental pore size distribution curves in Figs. 10 and 11 the quotients are the values of cos θ in column 6.

For N-291 the values of cos θ determined on the desorption side of the water isotherm are quite constant, with an average value of 0.49. The largest deviations come at relative pressures above 0.90 which may be partly due to greater errors in determining the slope of the curve (Fig. 8) in this region. The values of cos θ on the adsorption side are not as constant as on the desorption side and the greatest variation again comes at the higher relative pressures. The average value is 0.28.

For Darco G-60 the average value of cos θ on the desorption side of the isotherm is again 0.49, in good agreement with that for N-291.

The pore size distribution curves in Figs. 10 and 11, designated as being calculated by the Kelvin equation, were obtained by multiplying the pore diameters in column 5 of Tables I, II and III by the average value of cos θ. The great similarity between the calculated and experimentally determined pore size distribution curves shows graphically the constancy of cos θ, which is strong support for capillary condensation and the validity of the Kelvin equation.

TABLE I

CALCULATION OF MAGNITUDE OF COS θ FOR N-291 ON THE DESORPTION SIDE OF THE ISOTHERM

Pore volume, cc./cc.	Weight of water, g./cc.	Molar volume V	P/P_0	$\frac{4\sigma V}{RT \ln P_0/P}$	Cos θ
0.010	0.009	20.0	0.485	32.6	0.55
.020	.017	21.2	.508	36.7	.50
.040	.034	21.2	.525	37.3	.49
.060	.052	20.8	.534	39.1	.47
.080	.071	20.3	.540	38.9	.48
.100	.089	20.2	.545	39.2	.48
.120	.107	20.2	.547	39.5	.48
.140	.125	20.2	.550	39.8	.48
.160	.144	20.0	.553	39.9	.48
.180	.162	20.0	.556	40.6	.48
.200	.180	20.0	.560	40.7	.49
.220	.198	20.0	.567	41.5	.50
.230	.207	20.0	.577	42.9	.51
.240	.216	20.0	.620	49.3	.60
.245	.226	19.5	.800	103.0	.39
.246	.229	19.3	.897	190.0	.24
.247	.230	19.3	.960	552	.11
				Average except last two	.49

TABLE II

CALCULATION OF MAGNITUDE OF COS θ FOR N-291 ON THE ADSORPTION SIDE OF THE ISOTHERM

Pore volume, cc./cc.	Weight of water, g./cc.	Molar volume V	P/P_0	$\frac{4\sigma V}{RT \ln P_0/P}$	Cos θ
0.020	0.01	20.0	0.610	47.7	0.34
.040	.036	20.0	.650	54.8	.30
.060	.054	20.0	.672	59.4	.28
.080	.072	20.0	.690	62.4	.27
.100	.091	19.8	.703	66.2	.26
.120	.110	19.6	.715	69.0	.25
.140	.128	19.6	.725	72.1	.25
.160	.147	19.6	.735	75.2	.25
.180	.166	19.5	.745	77.9	.25
.200	.184	19.5	.755	81.6	.27
.220	.203	19.5	.770	88.1	.33
.230	.213	19.4	.787	95.7	.38
.245	.227	19.4	.850	140.0	.55
				Average except last one	.28

TABLE III

CALCULATION OF MAGNITUDE OF COS θ FOR DARCO G-60 ON THE DESORPTION SIDE OF THE ISOTHERM

Pore volume, cc./cc.	Weight of water, g./cc.	Molar volume V	P/P_0	$\frac{4\sigma V}{RT \ln P_0/P}$	Cos θ
0.010	0.080	22.5	0.335	24.3	0.41
.020	.016	22.5	.500	38.3	.39
.040	.033	21.8	.565	45.0	.51
.060	.053	20.4	.830	129.0	.58
.080	.073	19.7	.895	208	.59
.090	.083	19.5	.905	230	.59
.100	.093	19.3	.910	239	.58
.120	.113	19.1	.917	262	.54
.140	.133	18.9	.921	273	.54
.160	.153	18.8	.925	281	.54
.180	.173	18.7	.928	294	.53
.200	.193	18.65	.932	312	.50
.220	.213	18.6	.937	338	.48
.240	.233	18.55	.948	410	.42
.250	.243	18.5	.955	476	.37
.260	.253	18.5	.963	585	.34
.270	.263	18.5	.970	692	.40
.280	.273	18.45	.978	954	.47
				Average	.49

Theories of Capillary Condensation.—From the experimental evidence, which clearly indicates that we are dealing with capillary condensation in N-291 and Darco G-60, it is possible to arrive at some conclusions as to the causes of hysteresis observed in the water adsorption isotherms. The open pore hypothesis, as originally proposed by Cohan,[8] cannot be readily used to explain hysteresis in these charcoal systems. This is evident since presumably an adsorbed mon-

(8) Cohan, THIS JOURNAL, **60**, 433 (1938); *cf.* also *ibid.*, **66**, 98 (1944).

olayer is not formed on adsorption as required by the Cohan equation and since the equilibrium pressure for adsorption in open cylindrical capillaries given by that equation gives essentially the same value as the equilibrium pressure for desorption[9] as given by the Kelvin equation with $\cos \theta = 0.49$. The "bottle neck" hypothesis of Kraemer[10] or its modified form, the constriction hypothesis of McBain,[11] remains as a possible explanation.[12] An analysis of the experimental data has been made to learn how well the results meet the requirements of the constriction theory.

According to this hypothesis, as its name implies, the pores contain constrictions which have a pronounced effect on the equilibrium vapor pressure, depending on whether the equilibrium pressure is approached from the adsorption or desorption side. On the adsorption side of the hysteresis loop the vapor pressure is in equilibrium with menisci in the wider parts of the body of the pores between constrictions, while on the desorption side the vapor pressure is in equilibrium with menisci near the constrictions. The discussion of the adsorption and desorption processes may be facilitated with diagrams such as those presented in Fig. 12 which show a possible arrangement and relative sizes of the constriction and the body of the pore, or each section may represent separate pores.

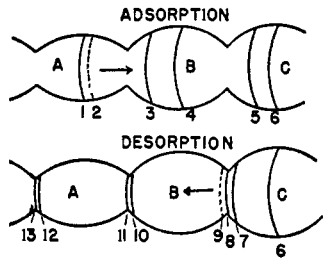

Fig. 12.—Diagrammatic representation of possible positions of menisci in constricted pores.

If the adsorption process is followed, starting at some point well up in the isotherm, it may be supposed that the relative vapor pressure is in equilibrium with meniscus 1 in body A. As more water is adsorbed the meniscus moves toward 2, but at 2 a metastable state is reached because the diameter here is less than at 1. There is a great tendency to fill up the narrow part of the pore to bring the meniscus to 3. From 3 to 4 the adsorption proceeds in a more normal fashion accompanied by an increasing relative vapor pressure. This same process is repeated between 4 and 6 and corresponding parts in larger pores.

(9) *Cf.* Fineman, Guest and McIntosh, *Can. J. Research*, **24B**, 109 (1946), who estimated pore radii by application of the Cohan equation to the adsorption branch of the water isotherm.

(10) Kraemer in H. S. Taylor's "A Treatise of Physical Chemistry," D. Van Nostrand and Co., Inc., New York, N. Y., 1931, Chapt. XX.

(11) McBain, THIS JOURNAL, **57**, 699 (1935).

(12) *Cf.* also Emmett and DeWitt, THIS JOURNAL, **65**, 1253 (1943); Emmett and Anderson, THIS JOURNAL, **67**, 1492 (1945); Cohan, THIS JOURNAL, **66**, 98 (1944).

Because the adsorption process, except for pores open directly to the atmosphere, ends with the meniscus in the body of the pore as, for example, at 6 in C, the desorption process may begin with a large decrease in relative vapor pressure which is proportional to the decrease in pore diameter in the body to the first largest constriction, as from 6 to 8. The main desorption branch and desorption scanning curves of the isotherm of N-291 and to a lesser extent of Darco G-60 have this characteristic. As more water is desorbed the meniscus moves toward 9 where a metastable state is reached and water in B will desorb until the meniscus is at a new equilibrium position at 10. From 10 to 11 the desorption proceeds normally, accompanied by a slight decrease in relative vapor pressure.

The significant implication of this concept of hysteresis associated with pore structure in the adsorption branch of the hysteresis loop is a measure of the order in which pores of increasing body diameter are filled and the desorption branch is a measure of the order in which pores of decreasing constriction diameter are emptied. If the order of the pores arranged in increasing body diameter is different from the order in increasing constriction diameter, the order in which the pores are filled on adsorption will not be the exact reverse of the order in which they will be emptied on desorption.

From this concept of adsorption and desorption processes it follows that the surface area–pore volume curve obtained for the desorption process, Fig. 8, gives the change in surface area as the pores are emptied in order of decreasing constriction diameters, while for the adsorption process it gives the change in surface area as the pores are filled in order of increasing body diameters. If the arrangement of pores in order of increasing body diameter had been the same as the order in increasing constriction diameters, the surface area–pore volume curves for the adsorption and desorption processes (Fig. 7) would have coincided. The difference between these two curves can be accounted for by this difference in order of arrangement of pores, since pores of small body diameters with relatively large constriction diameters, which fill first on adsorption and also empty first on desorption, have a larger surface area per unit volume than pores of large body diameters with relatively small constriction diameters, which fill last on adsorption and also empty last on desorption. By different arrangements of the order of increasing constriction and body diameters and different relative sizes of the constriction and body diameters it is possible to explain almost any shape of the hysteresis loop and scanning curves.

The curves in Figs. 10 and 11 are then the distributions of the average diameters of pores arranged in order of increasing constriction or body diameters. The calculated $\cos \theta$ values, 0.49 on desorption and 0.28 on adsorption, may then be

considered only as constants or factors which give the correct pore size distribution when substituted into the Kelvin equation and applied to the appropriate branch of the hysteresis loop. For a given P/P_0 this factor might be expected to vary in each pore volume range but the experimental value is an average over all the pore volumes since all the pores contain water to a given diameter but the smaller the pore the greater the depth to which it is filled and the more this diameter approaches the average diameter. The true cos θ, which may be associated with the contact angle or the ratio of attraction of water and carbon over intermolecular attraction, may then be the average of these two values, *i. e.*, 0.38. If cos θ = 0.38 is used in the Kelvin equation to calculate a pore size distribution from both sides of the experimental isotherm, the curves A and D in Fig. 13 are obtained. Curve A is the approximate distribution of the diameter of the pore bodies in the region between 3 and 4, and *D* is the approximate distribution of the diameters near the constrictions in the region between 10 and 11. These two curves show that the body diameters for this charcoal are roughly twice as large as the constriction diameters.

Acknowledgments.—In connection with the part of the work on pore structure done at the Division 10, NDRC Central Laboratory at Northwestern Technological Institute, the authors wish to express their thanks to Drs. W. C. Pierce, J. William Zabor, F. E. Blacet, Duncan MacRae, and other members of the NDRC staff who contributed to this work. The authors wish to thank the Chemical Corps Technical Command for the financial support which permitted continuation of the studies at the University of Rochester.

Summary

The pore structures of three charcoals were investigated. Charcoals N-291 and Darco G-60 were found to adsorb water only by capillary condensation while in PN-439 monolayer adsorption predominated.

The molar volume of the adsorbed water in the first two charcoals was determined by helium displacement measurements. By measuring the residual surface area of a charcoal containing varying amounts of water at different relative vapor pressures and from the variation of surface area as a function of volume of adsorbed water, assuming cylindrical pores, it was possible to calculate the pore diameter corresponding to any relative vapor pressure. On comparing the pore diameters determined in this way with those calculated with the Kelvin equation from the isotherm, values were obtained for cos θ, the contact angle. On the desorption side of the isotherm for both charcoals cos θ was 0.49 and on the adsorption side for N-291 cos θ was 0.28. The values were quite constant over practically the whole relative pressure range.

The hysteresis observed in the water isotherm seems to be explained most satisfactorily by the constriction hypothesis, according to which the adsorption side of the isotherm represents the order of increasing body diameters as the pores are filled and the desorption side the order of decreasing constriction diameters as the pores are emptied. Cos θ = 0.49 in the Kelvin equation when applied to the desorption side of the isotherm is a constant which will give the order of decreasing average pore diameters when the pores are emptied and likewise cos θ = 0.28 is a constant which will give the order of increasing average pore diameters when the pores are filled. The actual cos θ is probably an average of these two values.

RECEIVED JANUARY 10, 1949

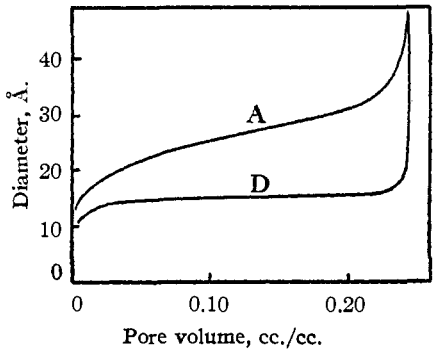

Fig. 13.—Pore size distribution in order of increasing constriction (D) and body (A) diameters; A, adsorption; D, desorption.